# A Comparative Study between Studs and PBLs on Mechanical Behavior of Composite Girders Subjected to Hogging Moment

W. Lin* and T. Yoda**

** Department of Civil and Environmental Engineering, Waseda University, Shinjuku-ku, Tokyo 169-8555, Japan (E-mail: linweiwei@aoni.waseda.jp)*
*** Department of Civil and Environmental Engineering, Waseda University, Shinjuku-ku, Tokyo 169-8555, Japan (E-mail:yoda1914@waseda.jp)*

## ABSTRACT
The purpose of the present study is to investigate an influence of different types of shear connectors on mechanical behaviour of composite steel and concrete girders under negative bending moment. Two overturned simply supported steel-concrete composite girders with different shear connectors including Studs and Perfo-Bond Strips (PBLs) were tested under point load in the mid-span. Based on the experimental observations, a three-dimensional FE model capable of analyzing the composite girders subjected to negative bending moment was built. Load and deformation response, concrete initial cracking and composite girder ultimate load bearing capacity, strain development process of reinforcing bars before and after concrete cracking were observed in the test and compared with the numerical values. Results predicted by this modelling method are in good agreement with those obtained from the tests. Furthermore, the "crack closure" or "through crack" load were recorded by π-gauges in the tests and compared with the code-specified ultimate load.

## KEYWORDS
Composite steel and concrete girder; Hogging moment; Studs; PBLs.

## INTRODUCTION
For continuous steel-concrete composite girders, the negative bending moment acting in the support regions will generate tensile stresses in the concrete slab and compressive stresses in the lower steel profile. As a result, the mechanical behavior of these girders is strongly nonlinear even for low stress levels, due not only to the slip at the beam-slab interface, but also the cracking in the slab, which generally has shortcomings in view of durability and service life of the structures. Besides, Studs and Perfo-Bond Strips (PBLs), generally known as flexible and rigid shear connectors separately, are most frequently-used shear connectors in composite girders. For this reason, this paper presents the experimental and numerical results of two composite girders subjected to negative bending. The objective of the present study is to clarify the difference between Studs and PBLs on inelastic mechanical behavior of composite girders subjected to negative bending moment.

## SUMMARY OF TESTS
### Details of test specimens
Two overturned simply supported composite beams of CBS and CBP were tested under concentrated load in mid-span. Each of the specimens was 4.6m in length and was simply supported at a span of 4m. The concrete slab thickness was 250mm with a width of 800mm. Different shear connectors, including 22mm nominal diameter headed shear studs and PBLs with the thickness of 12mm were used to connect the concrete slab and the steel girder in CBS and CBP respectively. The typical geometry of test specimen is shown in **Fig.1** and the details are illustrated in **Table.1**.

**Table.1** Details of test specimens

| Specimen | Connection device | Shear connectors spacing(mm) | | Reinforcing bars spacing (mm) | |
|---|---|---|---|---|---|
| | | Longitudinal spacing | Transverse spacing | Longitudinal bars | Stirrup |
| CBS | Stud | 150 | 100 | 100 | 150 |
| CBP | PBL | 150 | 240 | 100 | 150 |

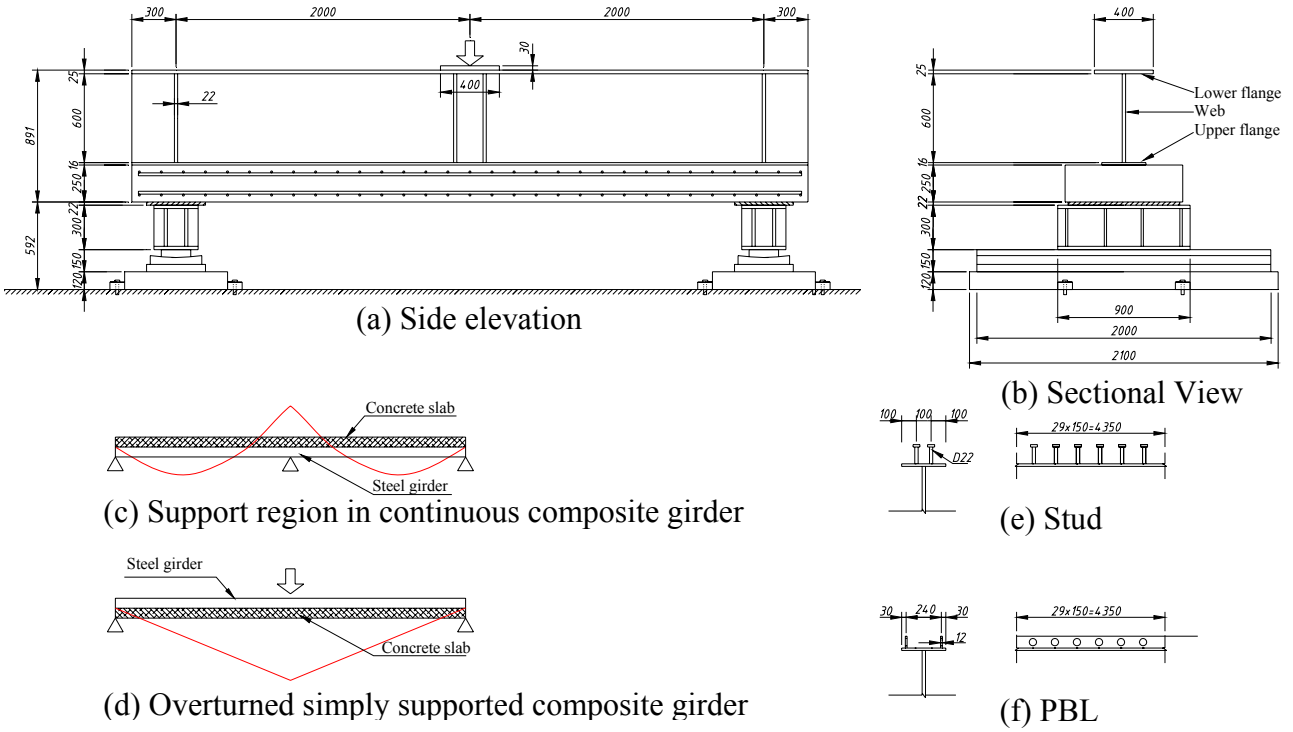


(a) Side elevation

(b) Sectional View

(c) Support region in continuous composite girder

(e) Stud

(d) Overturned simply supported composite girder

(f) PBL

**Fig.1** Dimensions of test specimen (mm)

**Instrumentations and test set-up**

Measurement of strains in the reinforcements, structural steel and concrete slab were conducted by means of electric resistance gauges at sections located at mid-span, 20cm and 60cm from the mid-span, respectively. Vertical deflections and transverse deformations were measured by mean of deformation gauges. Measurement of slip between the concrete slab and steel beams was conducted by means of deformation gauges, and the π-gauges for measuring the crack width on the concrete slab were also employed in the test. The test specimen was supported by a roller system at two ends. After the drying shrinkage had stabilized, pre-loading was applied to check the reliability of the measure equipment and the stability of the test specimen. The test girder was loaded in four cycles with the maximum loads of 200, 400, 700, 1300 kN before the ultimate load was reached. The loading was terminated when either the maximum stroke of the jack was reached or when the load capacity of the test specimen dropped significantly.

## 3. NUMERICAL SIMULATION OF EXPERIMENT

**Model building**

The modelling of each numerical model was carried out in three dimensions using the finite-element method and the *DIANA* software. Solid elements, shell elements, spring elements were used to simulate the concrete slab, steel girder and shear studs respectively. Also, in order to account for the slip between concrete slab and steel girder, interface elements were employed.

**Material properties**

*Concrete.* Material property of concrete was determined from material test. The nominal concrete compressive strengths and tensile strengths achieved after twenty-eight days of curing for CBS and CBP was (35.5, 2.50), and (29.1, 2.18) N/mm$^2$, respectively. The often quoted stress-strain curve due to Hognestad (Hognestad, 1951) was employed to simulate the compression behavior of concrete, shown in **Fig.2**. Experimental tension-stiffness curve proposed by Nakasu et al. (1996) are used to simulate the tension softening behavior of concrete.

*Structural steel and reinforcing bars.* The uniaxial stress-strain relationships for structural steel and reinforcing bars shown in **Fig. 3** were adopted in numerical models based on the material tests. Three steel beam coupons were cut out from different components of the upper flange, web, lower flange and PBL with different nominal thickness of 16, 22, 25 and 12mm respectively, and the tensile tests were performed. Fourteen reinforcing bars of D19 nominal diameter were used for two layers as longitudinal reinforcing bars in the concrete slab, whilst D13 stirrup reinforcing bars were used as torsional reinforcement with a nominal diameter of 13 mm.

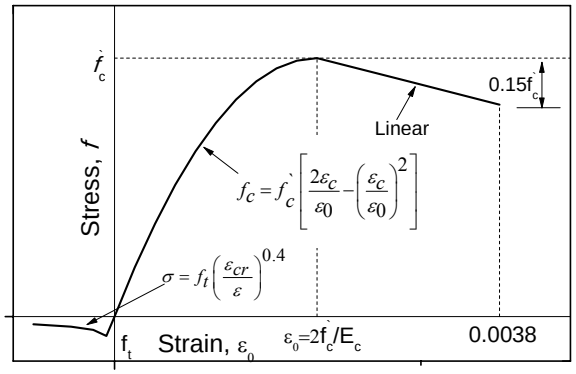


**Fig.2** Stress-strain curve for concrete

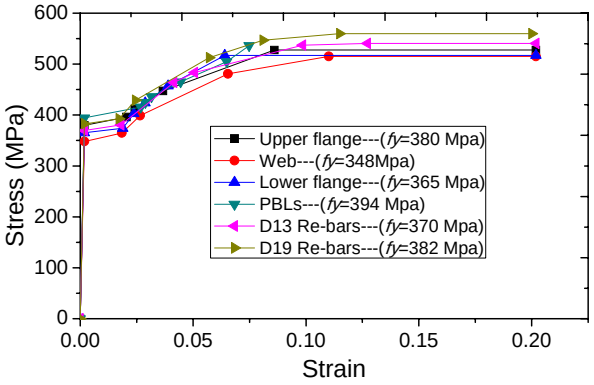


**Fig.3** Multi-linear relationship for steel and Re-bars

*Interface modelling.* Simplified interface property by considering the bond-slip model can be described as shown in **Fig.4**, which was used in this study to simulate the composite action between the concrete slab and steel girder. Based on previous comparison studies between experimental and numerical studies (Okada et al. 2004), the maximum shear bond stress was taken as 2.4 N/mm$^2$ due to the application of rubber-latex on the interface and the corresponding initial slip $\triangle u_t^0$ was taken as the standard value of 0.06mm suggested by Dörr et al. (1980).

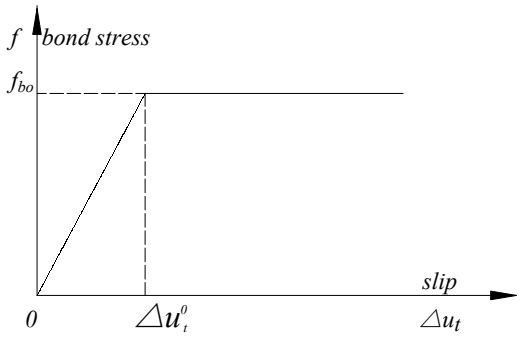


**Fig.4** Material properties of interface

*Shear connector.* PBLs are simulated by shell elements in the finite element model, and the material property is illustrated in **Fig. 3**. The shear studs were modelled by nonlinear spring elements. For each stud, three springs are used, two in horizontal direction and one in vertical direction. The constitutive relationship of the spring shown in **Fig.5** is given by **Eqn. (1)** (Ollgaard et al., 1971), in which the ultimate shear force loading capacity of studs was specified by JSCE specifications (2007).

$$Q=Q_u(1-e^{-0.7S})^{0.4} \quad (1)$$

$$Q_u = \min\begin{pmatrix} 31A_{ss}\sqrt{(h_{ss}/d_{ss})f_{cd}^{'}}+10000)/\gamma_b \\ A_{ss}f_{ss}/\gamma_b \end{pmatrix} \quad (2)$$

where $S$: slip of the shear stud (mm), $A_{ss}$: area of the shank of the stud (mm$^2$), $d_{ss}$: diameter of the shank of the stud (mm), $h_{ss}$: height of the stud (mm), $f_{cd}$: design compressive strength of concrete (N/mm$^2$) ($=f_{ck}/\gamma_c$), $f_{ck}$: the characteristic compressive strength of concrete (N/mm$^2$), $f_{ss}$: design tensile strength of the stud (N/mm$^2$) ($=f_{sk}/\gamma_s$), $f_{sk}$: characteristic tensile strength of the stud (N/mm$^2$), $\gamma_c$: material factor of concrete (=1.3), $\gamma_s$: material factor of stud (=1.0), $\gamma_b$: member factor (=1.3).

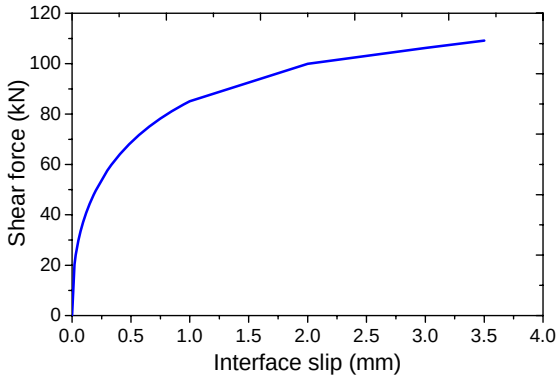


**Fig.5** Constitutive relation of shear stud

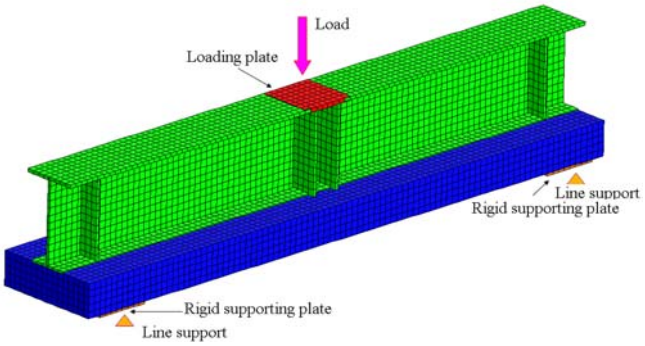


**Fig.6** FE model of test specimen

## RESULTS AND DISCUSSION

### Load and deflection response

The load-displacement curves obtained from the numerical analyses are compared with the experimental data as shown in **Fig.7**. Both numerical and experimental displacements are taken from the vertical deflection at the bottom mid-point of the composite beam, which is the bottom point of the concrete slab. The loads corresponding to the theoretical yield and full plastic moments are plotted as the horizontal lines indicated by $P_y$ and $P_p$, respectively. The ultimate pure bending moments, $M_{u,t}$ is to be calculated following the procedure for computing the plastic bending moment of composite sections under negative moment specified in Appendix D6.1 of AASHTO LRFD (2007).

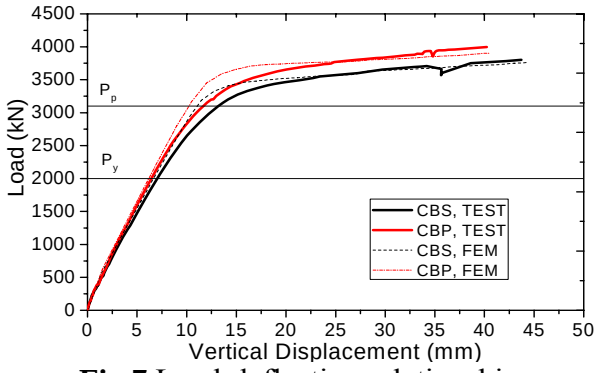


**Fig.7** Load-deflection relationship

It is found that in the linear region, the load-displacement curves from numerical studies agree well with the measured results. However in the nonlinear region after girder yielding, the rigidity of FE model is a little bit stronger than the test girder. This is presumably because the residual stress of steel girder is not considered in the finite element analysis, which may result in slightly larger stiffness of FE model than that of the test girder. At the final stage, the concrete can not sustain any increase in applied loading and eventually fails by through crack in the mid-span. The numerical results and experimental results are summarized and compared in **Table.2**.

The initial cracking load calculated with reference to the slab exhibiting maximum negative moment of composite section under elastic state has been estimated to be 247kN for both CBS and CBP, were close to numerical results but larger than experimental values. It seems to indicate that the initial cracking load is very small for composite beams under negative bending moment and thus making the structural behavior highly nonlinear even for very low stress levels. Regarding to the ultimate bending moment, as strain hardening of the steel girder and reinforcing bars were not considered in the theoretical analysis, resulting in that the experimental results was approximate to numerical results but much larger than the theoretical values. Moreover, comparison of load-deformation response of each specimen indicates that the displacement of CBP becomes a little less at around 1000kN than those of CBS, which is presumably because the PBL dowels affect the rigidity of the entire girder when cracking has progressed to a certain extent. Both experimental and numerical results indicate that the ultimate bending moment of CBP is larger than that of CBS.

**Table.2** Loading capacity of the test specimens

| Specimen | Initial cracking moment(kN.m) | | | Crack closure moment (kN·m) | Ultimate bending moment (kN·m) | | |
|---|---|---|---|---|---|---|---|
| | $M_{c,e}$ | $M_{c,t}$ | $M_{c,f}$ | $M_{c,c}$ | $M_{u,e}$ | $M_{u,t}$ | $M_{u,f}$ |
| CBS | 220 | 247 | 260 | 3500 | 3801 | 3104 | 3720 |
| CBP | 120 | 247 | 224 | 3203 | 3999 | 3104 | 3900 |

Note: $M_{c,e}$, $M_{c,t}$ and $M_{c,f}$ = Initial cracking bending moment from experiments, theoretical calculation and numerical values; $M_{c,c}$ = Crack closure bending moment from experiments; $M_{u,e}$,$M_{u,t}$ and $M_{u,f}$= ultimate bending moment from experiments, theoretical calculation and numerical calculation, respectively.

**Strain of reinforcements**

The strains of longitudinal reinforcements in the mid-span near the loading point were measured in the tests. **Fig.8** shows gauges' number (gauges 13, 15, 17 were arranged for the upper layer reinforcements, and gauge 43, 45, 47 were employed for the lower layer reinforcements) and locations. Strain development of the reinforcement before theoretical girder yielding load as well as the strain results during the whole loading process were illustrated separately. During the whole loading process, no obvious difference of numerical strain results was found between different reinforcements in the same layer, so average values for both upper and lower layers were given separately to compare with the test results. The strain increased linearly and slowly before the concrete slab cracking. After the initial cracking, the strain near the point where the crack has occurred increased rapidly (often referred to as strain jump). Similar phenomenon was also confirmed in the numerical studies, shown in **Fig.9 (a)** and **Fig.10 (a)**. In regard to the initial cracking moment, results in **Table.2** indicate that the numerical results agree well with the theoretical values, but larger than the test values. It demonstrates that for continuous composite steel and concrete structures, the concrete slab will crack and thus making the structural behavior highly nonlinear even for low stress levels.

Until the theoretical girder yielding load of the specimen, the reinforcements were continuously deformed and the strain of upper layer reinforcements was found larger than those of lower reinforcement. Comparison between numerical and theoretical results indicates that numerical strain results of reinforcements had a similar variation trend but a little bit smaller than test values, which might be caused by the initial cracks in the concrete slab that cannot be considered in the numerical simulation. Beside, as the concrete in tension zone are usually suggested to be ignored for ultimate strength calculation, resulting in theoretical yielding loads is smaller than the test values, as shown in **Fig.9** (b) and **Fig.10** (b)**.** The tension stiffening effect between cracks should be considered in order to evaluate the more exact flexural stiffness of the composite section under hogging moments.

Furthermore, as perfect bond was assumed between reinforcing bars and surrounded concrete, resulting in smaller strain during the loading process and deferred Re-bar yielding in the numerical

analysis. Also, strain hardening of the reinforcements was confirmed in the experiment for some reinforcements. However, for some other reinforcements, the strain was declined before strain hardening was obtained, which could be caused by the bond effect failure between the concrete and the reinforcement. Therefore, it seems that the strain hardening effect of reinforcement for composite girders in negative bending moment region can be ignored.

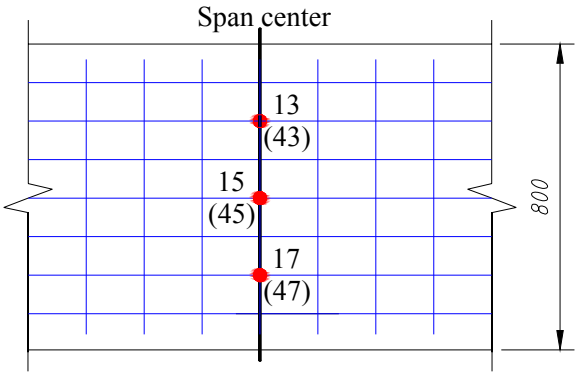


**Fig.8** Position of reinforcement strain gauges

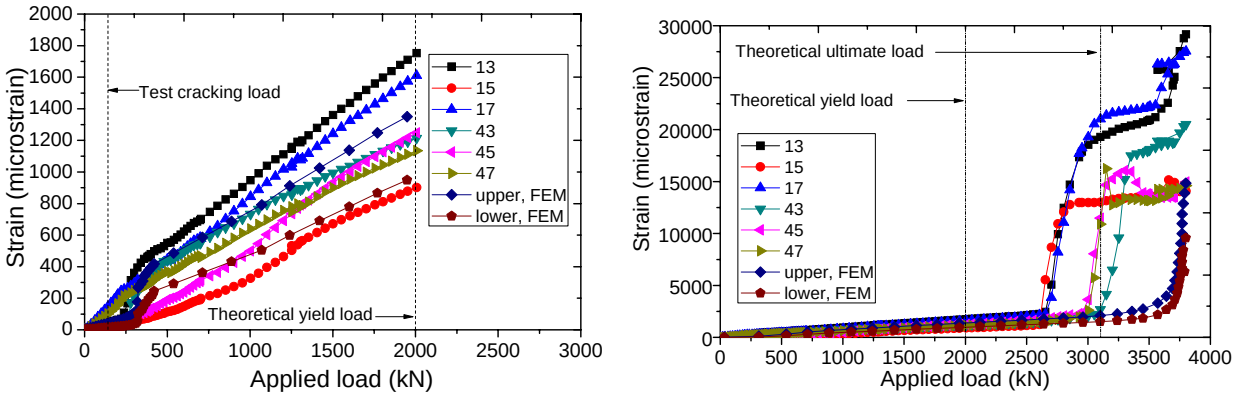


(a) P < 2000kN (b) whole loading process

**Fig.9** Strain development of reinforcing bars of CBS

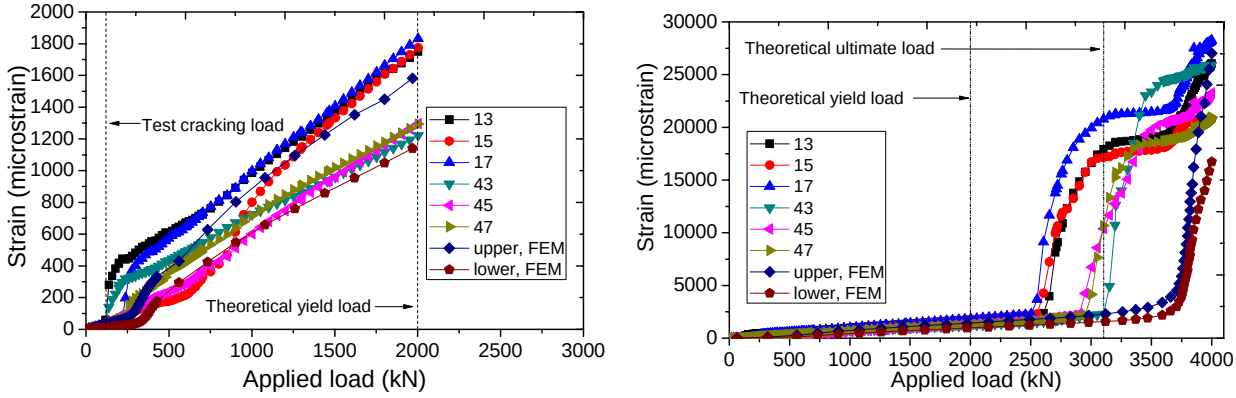


(a) P < 2000kN (b) whole loading process

**Fig.10** Strain development of reinforcing bars of CBP

**Crack formation and development on concrete slab**

Initial crack formation and crack width development during the loading process were recorded by using 14 π-gauges on the surface of the concrete slab. Numbers, locations as well as measurement of π-gauges in the experiments were shown in **Fig.11**. Crack width calculated by considering the maximum crack spacing (taken as 217mm according to JSCE, 2007) and Re-bars strains from

numerical models was illustrated as numerical results, shown in **Fig.12** and **Fig.13**, in which the average experimental values of crack width were also given to make a comparison.

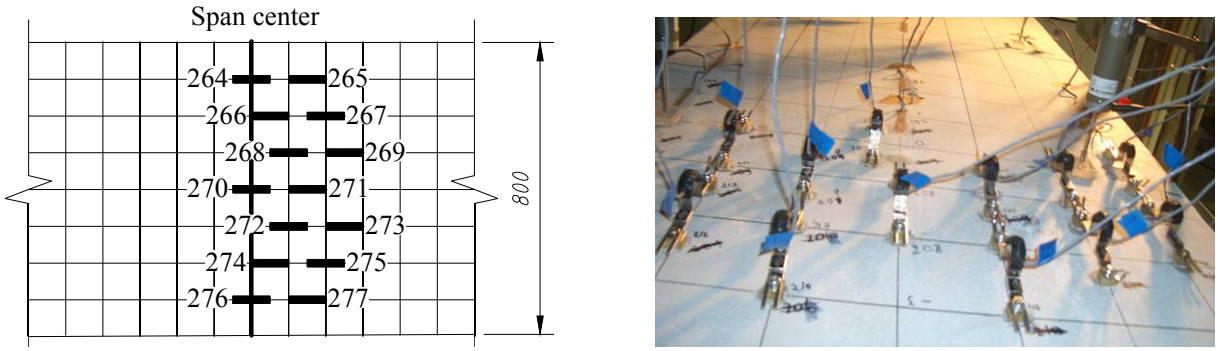


(a) π-gauge locations and gauge numbers (b) π-gauge arrangement in the test

**Fig.11** Arrangement of π-gauges (100mm square meshes on the concrete slab)

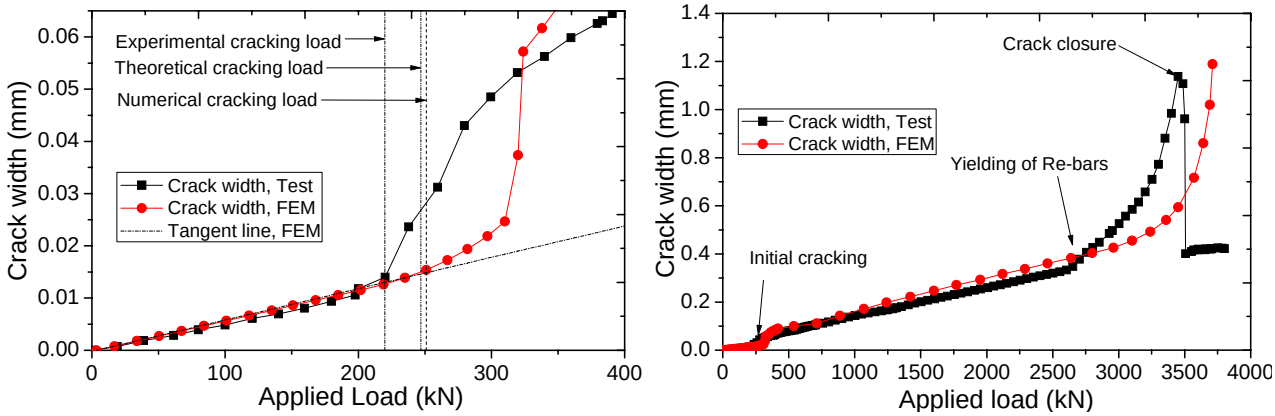


(a) Initial cracking (b) whole loading process

**Fig.12** Crack development process of CBS

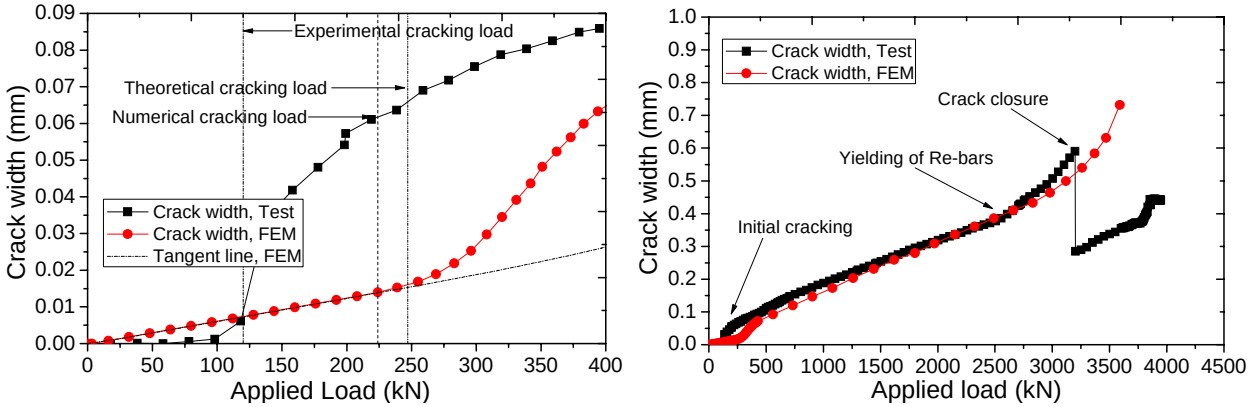


(a) Initial cracking (b) whole loading process

**Fig.13** Crack development process of CBP

The crack width jump shown in **Fig.12** (a) indicates that the initial cracks occurred at the top of concrete slab near loading position when applied load reached to 220kN, which is a little bit smaller than the numerical and theoretical results, as shown. **Fig.12** (b) also demonstrates that the proposed numerical model can simulate the un-cracked section well and give similar results to experimental values. However after initial cracking, experimental cracking width becomes larger than numerical values. The results shown in **Fig.12** (b) demonstrates that before Re-bar yielding, the assumption of perfect bond between Re-bars and surrounded concrete will not affect on crack width and the numerical simulation has similar results in comparison with test values. Also, the results indicate that the smeared crack model that usually used in commercial software is capable for simulating the

crack development process. However after Re-bar yielding, non-ignorable slip is produced between Re-bars and concrete, resulting in larger difference between numerical and experimental results.

In addition, an interesting phenomenon of "crack closure" was observed in the test for both CBS and CBP, and the crack width was found suddenly to become small and to keep constant for all large cracks before the ultimate load was reached, shown as **Fig.12** (b) and **Fig.13** (b). This might be because the sectional through crack was generated and the bond effect between the concrete slab and the steel girder was failure, thus the concrete slab lost its loading capacity and the crack width just remains stable. Due to the strain hardening of the steel girder, the composite girder could sustain more loads after the "crack closure" was observed. However, as the concrete had through cracks, the girder stress as well as its deformation increased rapidly until the ultimate load was reached. Nevertheless, similar phenomenon cannot be found in the numerical analysis, which was due to perfect bond assumption between reinforcing bars and surrounding concrete.

## CONCLUSIONS

The results indicate that both PBL and stud connectors are effective shear connective devices for composite girders subjected to negative bending moment, and no obvious differences were found except that PBL connectors could slightly improve the rigidity of the composite girder in both the serviceability limit state and the ultimate limit state in comparison with stud connectors. Stud specimens have relatively better mechanical behavior in regard to concrete slab cracking behavior, such as initial cracking and crack closure. Besides, the proposed numerical models can simulate the test specimens and can be served as a basis for the design of composite bridges under negative bending moment. Perfect bond assumption for concrete-reinforcement interface was proved suitable before re-bar yielding.

## ACKNOWLEDGEMENT

The financial support sponsored by Ministry of Land, Infrastructure, Transport and Tourism of Japan is gratefully acknowledged. The financial support from China Scholarship Council for the first author was also gratefully appreciated.

## REFERENCES

AASHTO. (2007). *AASHTO LRFD Bridge Design Specifications*, Washington, DC.

DÖRR, K. (1980). Ein Beitrag zur Berechnung von Stahlbetonscheiben unter besonderer Berücksichtigung des Verbundverhaltens. PhD thesis, University of Darmstadt.

Hognestad, E. (1951). *A study of combined bending and axial load in reinforced concrete members*, University of Illinois Engineering Experiment Station. Bulletin Series, 3.

Japan Society of Civil Engineers (JSCE). (2007). *Standard specifications for steel and composite structures*.

Nakasu, M., and Iwatate, J. (1996). *Fatigue experiment on bond between concrete and reinforcement*, Transaction of JSCE, Vol 426, 852-53.

Okada, J., Yoda, T., and Lebet, J.P. (2004). *A study of the grouped arrangement of stud connectors on the shear strength*, Journal of the Japan Society of Civil Engineers, Vol 766, 81-95.

Ollgaard, J.G., Slutter, R.G., Fisher, J.W. (1971). *Shear Strength of Stud Connectors in Lightweight and Normal Weight Concrete*. Engineering Journal of AISC, **8**(2): 55-64.